0026-895X/07/7206-1466–1475$20.00
MOLECULAR PHARMACOLOGY
Copyright © 2007 The American Society for Pharmacology and Experimental Therapeutics
Mol Pharmacol 72:1466–1475, 2007

Vol. 72, No. 6
39040/3276901
Printed in U.S.A.

Mitochondria, Calcium, and Calpain are Key Mediators of Resveratrol-Induced Apoptosis in Breast Cancer

Dhruv Sareen, Soesiawati R. Darjatmoko, Daniel M. Albert, and Arthur S. Polans

Departments of Biomolecular Chemistry (D.S., A.S.P.) and Ophthalmology and Visual Sciences (D.S., S.R.D., D.M.A., A.S.P.), and the Paul P. Carbone Comprehensive Cancer Center (D.M.A., A.S.P.), University of Wisconsin School of Medicine and Public Health, Madison, Wisconsin

Received June 13, 2007; accepted September 10, 2007

ABSTRACT

Resveratrol (RES), a natural plant polyphenol, has gained interest as a nontoxic chemopreventive agent capable of inducing tumor cell death in a variety of cancer types. However, the early molecular mechanisms of RES-induced apoptosis are not well defined. Using the human breast cancer cell lines MDA-MB-231 and MCF-7, we demonstrate that RES is antiproliferative and induces apoptosis in a concentration- and time-dependent manner. Preceding apoptosis, RES instigates a rapid dissipation of mitochondrial membrane potential by directly targeting mitochondria. This is followed by release of cytochrome *c* and second mitochondria-derived activator of caspase/direct inhibitor of apoptosis-binding protein with low pI (Smac/DIABLO) into the cytoplasm and substantial increase in the activities of caspases-9 and -3 in MDA-MB-231 cells. In addition, live cell microscopy demonstrates that RES causes an early biphasic increase in the concentration of free intracellular calcium ($[Ca^{2+}]_i$), probably resulting from depletion of the endoplasmic reticulum stores in breast cancer cells. In caspase-3–deficient MCF-7 cells, apoptosis is mediated by the Ca^{2+}-activated protease, calpain, leading to the degradation of plasma membrane Ca^{2+}-ATPase isoform 1 and fodrin; the degradation is attenuated by buffering $[Ca^{2+}]_i$ and blocked by calpain inhibitors. Mitochondrial permeability transition pore antagonists also blocked calpain activation. In vivo mouse xenograft studies demonstrate that RES treatment inhibits breast cancer growth with no systemic toxicities. Together, these results suggest a critical role for mitochondria not only in the intrinsic apoptotic pathway but also in the Ca^{2+} and calpain-dependent cell death initiated by RES. Thus, RES may prove useful as a nontoxic alternative for breast cancer treatment.

Despite earlier diagnosis and aggressive therapeutics, breast cancer remains a leading cause of death among women. The chance of developing invasive breast cancer during a woman's lifetime is approximately 1 in 8, and more than 40,000 women die of metastatic disease each year (Jemal et al., 2006). Inherent or acquired tumor drug resistance limits many agents used in the treatment of this disease. In addition, these cytotoxic agents are often associated with severe, dose-limiting, systemic toxicities. Therefore, the need for development of novel nontoxic therapeutic agents active against breast cancer remains an important goal.

Basic and preclinical research on resveratrol [RES (*trans*-3,4′,5-trihydroxystilbene)], a naturally occurring polyphenol enriched in grapes and red wine, has shown pleiotropic cardioprotective, antiaging, and anticancer activities (Savouret and Quesne, 2002; Aggarwal et al., 2004; Bradamante et al., 2004). RES has been shown to inhibit tumor initiation, promotion, and progression in a variety of cell culture systems, including breast cancer cells (Jang et al., 1997; Bhat et al., 2001). It is noteworthy that RES suppresses in vivo tumor growth in xenograft and mutagen-induced animal models of mammary carcinogenesis (Banerjee et al., 2002; Garvin et al., 2006). Preliminary studies in our laboratory suggest that RES is effective in preventing tumor growth in neuroblas-

This work was supported by National Institutes of Health grant R01-CA103653 (to A.S.P.) and grants from the Retina Research Foundation (to A.S.P.), the Mandelbaum Cancer Theraputics Initiative (to A.S.P. and D.M.A.), and National Institutes of Health core grant P30-EY016665-02.

Article, publication date, and citation information can be found at http://molpharm.aspetjournals.org.

doi:10.1124/mol.107.039040.

ABBREVIATIONS: RES, resveratrol; PMCA, plasma membrane Ca^{2+}-ATPase; ER, endoplasmic reticulum; $\Delta\Psi_m$, mitochondrial membrane potential; mPTP, mitochondrial permeability transition pore; DMSO, dimethyl sulfoxide; Smac/DIABLO, second mitochondria-derived activator of caspases/direct IAP binding protein with low pI; Ac-, *N*-acetyl-; AFC, amino-4-trifluoromethylcoumarin; AMC, amino-4-methylcoumarin; Z-, *N*-benzyloxycarbonyl-; ROI, region of interest; CsA, cyclosporin A; CICR, Ca^{2+}-induced Ca^{2+} release; S-LLVY-AMC, succinyl-Leu-Leu-Val-Tyr-7-amino-4-methylcoumarin; JC-1, 5,5′,6,6′-tetrachloro-1,1′,3,3′-tetraethyl-benzamidazolocarbocyanin iodide; FCCP, carbonyl cyanide-*p*-(trifluoromethoxy)phenylhydrazone; BAPTA-AM, 1,2-bis(o-aminophenoxy)ethane-*N*,*N*,*N*′,*N*′-tetraacetic acid-acetoxymethyl ester; CHAPS, 3-[(3-cholamidopropyl)dimethylammonio]propanesulfonate; AM, acetoxymethyl ester; TG, thapsigargin; PD 150606, (2*S*)-3-(4-iodophenyl)-2-sulfanylpropanoic acid; SJA 6017, *N*-(4-fluorophenylsulfonyl)-L-valyl-L-leucinal; MDL 28170, *N*-benzyloxycarbonyl-Val-Phe-aldehyde.

toma and uveal melanoma murine xenograft models. Nevertheless, the precise mechanisms by which RES confers inhibition of tumor growth in vivo have not been well elucidated. In vitro studies on human cancer cell lines revealed that RES initiates antiproliferative and/or pro-apoptotic actions (Savouret and Quesne, 2002). The pro-apoptotic effect of RES has been attributed to downstream events activated after binding to putative cell surface receptors, including integrin $\alpha V\beta 3$ and sulfonylurea receptor isoform 1 (Lin et al., 2006; Hambrock et al., 2007). In addition, RES targets several enzymes involved in carcinogenesis, suggesting that multiple signaling cascades may be activated or inhibited depending on the cellular background (Sareen et al., 2006).

Apoptosis requires the participation of intracellular zymogens that systematically dismantle the cell via two distinct pathways. Activated caspase-8 (extrinsic death-receptor pathway) and activated caspase-9 (intrinsic mitochondrial pathway) both activate the executioner caspase-3, which in turn activates the degradation phase of apoptosis (Ashkenazi and Dixit, 1998; Green and Reed, 1998). There is evidence that RES can induce apoptosis through both mechanisms, although the absence of functional capase-3 in MCF-7 breast cancer cells indicates that alternative mechanisms may be involved (Delmas et al., 2003; Mohan et al., 2006; Sareen et al., 2006). In a separate intrinsic apoptotic pathway, alterations in Ca^{2+} homeostasis involving the ER can cause a stress response. In resting cells, the concentration of Ca^{2+} in the extracellular milieu and in the ER is relatively high (in the millimolar range). In contrast, the cytoplasmic Ca^{2+} concentration is maintained at ~100 nM by active extrusion from the cell by plasma membrane Ca^{2+}-ATPases (PMCA), plasma membrane Na^+/Ca^{2+} exchangers, and active uptake of cytosolic Ca^{2+} into the ER and mitochondria by distinct Ca^{2+}-ATPases and transporters, respectively. During elevated levels of cytosolic Ca^{2+} the mitochondrial membrane potential ($\Delta\Psi_m$) drives Ca^{2+} uptake into the mitochondria. Under conditions of stress, de-energized mitochondria release Ca^{2+} back to the cytosol via different mechanisms, opening of the mitochondrial permeability transition pore (mPTP) being one (Orrenius et al., 2003). Loss of Ca^{2+} homeostatic control either by release from the ER and mitochondria or influx through plasma membrane channels leads to sustained levels of cytosolic Ca^{2+} and cell death. However, the mechanisms that couple changes in cellular Ca^{2+} to apoptotic cell death in response to RES have been elusive and, in particular, the apoptosis-related Ca^{2+} targets have not been identified.

Although the best characterized proteases in apoptosis are caspases, other proteases, including calpains and cathepsins, contribute to apoptosis in the absence of caspase activation (Harwood et al., 2005). The Ca^{2+}-dependent cysteine proteases, *m*- and μ-calpains, are frequently activated in apoptosis models involving elevated $[Ca^{2+}]_i$. Calpain substrates include membrane receptors and transporters, cytoskeletal proteins, and intracellular enzymes. In particular, there is evidence that proteolysis of plasma membrane Na^+/Ca^{2+} exchanger 3 by calpain plays a prominent role in the delayed and irreversible Ca^{2+} elevation leading to neuronal demise (Bano et al., 2005). However, the mechanisms of cellular calpain activation during apoptosis are not well understood, and little is known about the involvement of calpains in tumor cell death.

In this study, we sought to investigate the early and pivotal intracellular apoptotic signaling mechanisms in MDA-MB-231 (caspase-3 positive) and MCF-7 (caspase-3 negative) breast cancer cells in response to RES. We demonstrate that RES significantly inhibits tumor growth in a xenograft model of breast cancer. In vitro and in vivo data show that RES induces mitochondrial depolarization and a transient spike in $[Ca^{2+}]_i$, followed by a secondary gradual rise in $[Ca^{2+}]_i$ contributing to an irreversible commitment to undergo the execution phase mediated by caspases and calpains. We show that the intrinsic mitochondrial caspase-dependent apoptotic pathway is activated in MDA-MB-231 cells. In addition to this caspase-dependent pathway, elevated $[Ca^{2+}]_i$ is induced by RES in both MDA-MB-231 and MCF-7 cell lines. This leads to activation of calpain and the subsequent proteolysis of in vivo substrates, including fodrin and PMCA1. The later events are more readily observed in the caspase-deficient MCF-7 cells.

Materials and Methods

Materials. The human breast cancer MCF-7 and MDA-MB-231 cell lines were obtained from Dr. Elaine Alarid (University of Wisconsin, Madison, WI). RES purchased from Cayman Chemicals (Ann Arbor, MI) was dissolved in sterile DMSO and further diluted in cell culture media. Mouse monoclonal antibodies were purchased for GAPDH from Biogenesis Inc. (Poole, UK), cytochrome oxidase subunit IV (clone 12C4) from Invitrogen (Carlsbad, CA), cytochrome *c* (clone 7H8.2C12) from BD PharMingen (San Diego CA), Smac/DIABLO from Cell Signaling Technology (Danvers, MA), α-fodrin (clone AA6) from BIOMOL International LP (Plymouth Meeting, PA), apoptosis-inducing factor (E-1) from Santa Cruz Biotechnology (Santa Cruz, CA). Rabbit polyclonal PMCA1 antibody was obtained from Affinity Bioreagents (Golden, CO). All other common reagents were procured from Sigma Chemical Co. (St. Louis, MO).

Cell Culture. MDA-MB-231 and MCF-7 cells were grown in Dulbecco's modified Eagle's medium, supplemented with 10% (v/v) fetal bovine serum, 2 mM L-glutamine, 100 units/ml penicillin G, 100 mg/ml streptomycin sulfate, and 0.25 mg/ml amphotericin B. Cultures were maintained at 37°C in 95% O_2/5% CO_2.

Breast Cancer Xenograft Study. Female athymic *nu*/*nu* mice, ~6 weeks of age (Harlan Sprague-Dawley, Indianapolis, IN), were housed in a pathogen-free isolation facility. Animal care and treatment protocols were approved by the University of Wisconsin-Madison Research Animals Resources Center. MDA-MB-231 cells were harvested, 5×10^6 cells resuspended in 500 μl of 1:1 culture media and basement membrane matrix (Matrigel; BD Biosciences, San Jose, CA) and injected subcutaneously into the dorsal flanks of 72 mice. After the tumors were established (150 mm^3), the animals were randomized into control and treatment groups (n = 36 mice per group). Control group animals were administered 0.1 ml of Neobee M5 oil alone, and treatment group animals received 50 mg/kg resveratrol in 0.1 ml of Neobee M5 oil by oral gavage daily for 5 weeks. Twice weekly during the treatment, each animal was weighed and the tumor volume was determined by measuring tumor size in three dimensions using calipers. Toxicity was assessed by survival, activity, and changes in body weight. At the completion of 5 weeks of treatment, the mice were euthanized; tumors, lungs, and livers were fixed in 10% neutral buffered formalin for histopathologic processing. Five-micrometer sections were cut and stained with hematoxylin & eosin for light microscopic analysis.

Tumor Cell Viability. MCF-7 and MDA-MB-231 cells were seeded in 96-well plates for 2 days and incubated with either DMSO or RES for a period of 1 to 7 days. At the end of the treatment, CellTiter-Blue dye was added according to the manufacturer's instructions (Promega, Madison, WI). Fluorescence was measured at excitation/emission wavelengths of 560/590 nm, using a fluorescence

plate reader (GE Healthcare, Chalfont St. Giles, Buckinghamshire, UK).

Cell Cycle Distribution Analysis. Propidium iodide staining was used to analyze DNA content on a flow cytometer (BD Biosciences FACstation) equipped with cell cycle analysis software, using standard procedures (Sareen et al., 2006).

Determination of Apoptotic Cell Morphology. MCF-7 and MDA-MB-231 cells were seeded into eight-well LabTek II chamberslides (Nalge Nunc International, Rochester, NY) and treated with 100 μM RES. At the end of the treatment, cells were fixed, washed, and stained with 1 μg/ml Hoechst 33528 (Invitrogen), using standard procedures (Sareen et al., 2006). Cells were viewed under a fluorescence microscope (Carl Zeiss, Oberkochen, Germany) using a 4,6-diamidino-2-phenylindole filter set, and apoptotic cells were counted.

Isolation of Mitochondria. Mitochondria from MCF-7 and MDA-MB-231 cells were isolated using a Potter-Elvehjem homogenizer according to previously published methods (Sareen et al., 2006).

Mitochondrial Transmembrane Potential. Changes in mitochondrial membrane potential from whole cells and isolated mitochondria were analyzed on a Shimadzu RP 5301-PC spectrofluorometer (Shimadzu Scientific, Columbia, MD) using the mitochondria-selective dye JC-1 (Cell Technology, Mountain View, CA), as described previously (Sareen et al., 2006).

Cytochrome *c* and Smac/DIABLO Release. Cytosolic and mitochondrial extracts were analyzed for cytochrome *c* and Smac/DIABLO content by immunoblotting, as described previously (Pozo-Guisado et al., 2005; Sareen et al., 2006). Protein concentration of the fractions was determined using the Bio-Rad protein assay kit (Bio-Rad Laboratories, Hercules, CA). Purity of the cytosolic fraction was confirmed by immunostaining with a mitochondria-specific marker, cytochrome oxidase subunit IV. GAPDH, a cytoplasmic protein, served as a control for protein loading.

Determination of Caspase Activation. MCF-7 and MDA-MB-231 cells were seeded on 10-cm culture dishes, treated with vehicle, RES, or additional apoptotic stimuli, and the activities of caspases-2, -3, -8, and -9 determined as described previously (Mohan et al., 2006; Sareen et al., 2006). In brief, at the end of treatment, cells were sedimented and resuspended in lysis buffer [10 mM Tris-HCl, 10 mM NaH_2PO_4, pH 7.5, 130 mM NaCl, and 1% (v/v) Triton X-100], and protein concentration was measured (Bio-Rad Laboratories). Subsequently, incubation of 80 μg of protein with caspase-9 substrate (Ac-LEHD-AFC; MP Biomedicals, Irvine, CA), 40 μg of protein with caspase-3 substrate (Ac-DEVD-AMC; BD PharMingen), 100 μg of protein with caspase-2 susbtrate (Z-VDVAD-AFC; EMD Biosciences), or 100 μg of protein with caspase-8 substrate (Z-IETD-AFC; EMD Biosciences) was performed in reaction buffer (100 mM HEPES, 1 mM EDTA, pH 7.1, 0.1% CHAPS, 10% glycerol, and 20 mM dithiothreitol) for 60 min at 37°C. Fluorescence of free AFC and AMC was monitored on a spectrofluorometer at excitation/emission wavelengths of 400 nm/505 nm and 380 nm/440 nm, respectively.

Intracellular Calcium Imaging. Changes in $[Ca^{2+}]_i$ were assessed using the cell permeant Ca^{2+}-sensitive ratiometric fluorescent indicator dye fura-2-AM (Invitrogen), as described previously (Robinson et al., 2004). In brief, MCF-7 and MDA-MB-231 cells seeded in 96-well imaging plates (BD Biosciences, San Jose, CA) were rinsed twice in buffer (5.9 mM KCl, 1.4 mM $MgCl_2$, 10 mM HEPES, 1.2 mM NaH_2PO_4, 5 mM $NaHCO_3$, 140 mM NaCl, 11.5 mM glucose, 1.8 mM $CaCl_2$, and 3 mg/ml bovine serum albumin, pH 7.3) and loaded with 8 μM fura-2 AM in loading buffer at 37°C for 30 min. After 30-min room-temperature incubation to allow for hydrolysis of the AM-ester, cells were rinsed in physiological salt solution, composed of loading buffer lacking BSA. BAPTA-AM (20 μM; EMD Biosciences, San Diego, CA) was coloaded with fura-2-AM where indicated. Dilutions of RES, TG, and DMSO were made in physiological salt solution. Serial acquisition of fluorescent images of cells were performed in a nonconfocal mode on a BD Pathway Bioimager system (BD Biosciences Bioimaging Systems, Rockville, MD), equipped with a temperature- and CO_2-regulated environmental chamber, a liquid-handling single-channel pipettor with image-as-you-add capabilities, and a 20× plan-fluorite objective (20× LUC Plan FLN; numerical aperture, 0.45; Olympus, Tokyo, Japan). Fura-2-AM was alternately excited at wavelengths of 340 and 380 nm, and emitted fluorescence was collected via a 510 nm band pass filter at each UV wavelength with an internal high resolution Hamamatsu ORCA ER cooled charge-coupled device camera (Hamamatsu Photonics, Japan). Basal images were collected for 25 s before drug addition. Subsequently, images were collected after the indicated treatments at 2.5 s intervals. $[Ca^{2+}]_i$ maps for individual cells were calculated after pixel-by-pixel computerized ratiometric reconstruction of individual images acquired using Attovision 5.0 three-dimensional imaging software. Calibration of the fluorescent signal was performed with fura-2 penta-K^+ salt using the two-point calibration procedure of imaging positive (10 μM fura-2 + 1 mM $CaCl_2$) and negative (10 μM fura-2 + 1 mM EGTA-Na) calcium standards. Software assisted ratio to $[Ca^{2+}]_i$ transformation was performed using the Grynkiewicz equation (Grynkiewicz et al., 1985).

Calpain Activity. Calpain activity in intact cells was monitored using a Shimadzu RP 5301-PC spectrofluorometer (Shimadzu Scientific, Columbia, MD) by measuring Ca^{2+}-dependent and calpain specific hydrolysis of the peptidyl 7-amino bond of the cell-permeable fluorogenic calpain substrate, S-LLVY-AMC (Sigma) (Potter et al., 1998). Previous studies have demonstrated that this assay is linear with cell number and the activity measured is representative of *m*- and μ-calpain activities observed with protein substrates (Sasaki et al., 1984; Guttmann and Johnson, 1998). In brief, cells from confluent dishes were harvested with 0.25% trypsin-EDTA solution, neutralized with 10% fetal bovine serum containing media, and washed twice with HEPES-buffered Hank's balanced salt solution, pH 7.4, without phenol red. Equal numbers of cells per assay were resuspended in HEPES-buffered Hank's balanced salt solution at 2.5×10^5 cells/ml and prewarmed at 37°C in a 5% CO_2 incubator for 10 min. Wherever indicated, the intracellular Ca^{2+}-chelator BAPTA-AM (20 μM), the cell-permeable μ- and *m*-calpain inhibitors PD 150606 (50 μM; selectively blocks the Ca^{2+} binding sites), SJA 6017 (50 μM; active site inhibitor), and MDL 28170 (25 μM; active site inhibitor) and the mPTP inhibitor cyclosporin A (CsA; 20 μM) (EMD Biosciences) were pretreated in the cell suspension, mixed, and incubated at 37°C for 30 to 45 min. To assay calpain activity, RES (100 μM final concentration) or DMSO vehicle was added to untreated or pretreated cell suspension (2.5×10^5 cells) 1 min before S-LLVY-AMC (25 μM) addition. AMC fluorescence was measured and calpain activity plots obtained at various time points on the spectrofluorometer with the excitation/emission wavelengths of 360 nm/400 to 500 nm. The initial rate of substrate cleavage, which was linear, was measured at 5 to 15 min after substrate addition. Trypan blue exclusion was used to ensure that the cells remained viable through the procedure.

Immunoblotting. Cultures were washed twice with PBS and lysed in ice-cold lysis buffer (50 mM Tris-HCl, pH 7.5, 150 mM NaCl, 0.5% Nonidet P-40, 1 mM PMSF, 1 mM NaF, 1 mM dithiothreitol, and 4 mg/ml complete protease inhibitor cocktail). Protein concentration was determined in cell lysates using the Bio-Rad protein assay kit. Aliquots of protein were mixed with SDS sample buffer and Western blot analysis performed using standard protocols (Sareen et al., 2006).

Results

Resveratrol Inhibited Tumor Growth in Athymic Nude Mice. We examined the effect of resveratrol on human breast cancer tumor growth in vivo by ectopic implantation of MDA-MB-231 cells into athymic nude mice. After 5 weeks of oral drug treatment, tumor growth in the RES-fed group,

compared with the control groups that were fed vehicle alone, was inhibited by 51% ($p = 0.003$) (Table 1). RES treatment had no effect on body weight and diet consumption during the 5 weeks of the experiment. No other signs of systemic toxicity or any adverse health effects as monitored by activity and posture of mice were observed. Furthermore, liver sections from RES-treated mice showed no evidence of abnormal pathology compared with those from controls. In addition, 14% (5/36) of the mice in the MDA-MB-231 RES-treated group showed regression of tumor size relative to the initial tumor volume (data not shown).

Resveratrol Displayed Dose- and Time-Dependent Proapoptotic and Antiproliferative Effects in Breast Cancer Cells. To examine the antitumor activity of RES in human breast cancer cells, exponentially dividing MDA-MB-231 and MCF-7 cells were treated with increasing concentrations of RES, and cell viability was measured over time. RES caused marked growth inhibition and significantly decreased the viability of MDA-MB-231 cells (IC_{50} at 48 h = 128.8 μM) and MCF-7 cells (IC_{50} at 48 h = 151.8 μM) in a time- and concentration-dependent manner compared with the DMSO-treated control (Fig. 1A). At 100 to 200 μM RES, there was a regression in the number of viable cells (Fig. 1A; compare days 1 and 7). The cytotoxicity caused by RES may be due in part to antiproliferative and proapoptotic effects. Consequently, the effect of RES on cell cycle progression was analyzed by flow cytometry in exponentially dividing cultures of MDA-MB-231 and MCF-7 cells treated with either DMSO or RES, and the percentages of cells in G_0/G_1, S, and G_2-M phases were calculated (Fig. 1B). RES caused an accumulation of cells in the S phase of the cell cycle for both cell lines [MDA-MB-231 (21% in control versus 70% and 71% with 50 and 100 μM RES, respectively) and MCF-7 (47% in control versus 70% with 50 μM RES)] with a concomitant decrease in the population of cells in the G_0/G_1 phase, indicative of a late S phase or early $G_{2\text{-}M}$ block. It is noteworthy that at 100 μM RES, the population of MCF-7 cells in G_0/G_1 increased to 54%, whereas cells in G_2-M decreased to 2%, suggestive of an early S phase block. These data are consistent with previous observations from other groups (Aggarwal et al., 2004; Kim et al., 2004). The block in cell cycle progression, therefore, contributes to RES-induced antiproliferative effects. In addition, there was a significant increase in the sub-G_1 fraction (hypodiploid DNA content) in both cell lines, possibly due to DNA fragmentation, resulting in an increase in RES-induced apoptotic cell death (data not shown). Subsequently, the ability of RES to cause MDA-MB-231 and MCF-7 cell apoptosis was determined by examining nuclear morphological changes with fluorescence microscopy. Cells that exhibited typical morphological features of apoptosis, such as chromatin condensation and pyknotic nuclei, increased in a time-dependent manner when treated with RES. Results are represented as percentage of apoptotic cells, which increased from 1.3% and 0.9% in control to 52% and 45% in RES treated MDA-MB-231 and MCF-7 cells, respectively (Fig. 1C), suggesting that RES has a proapoptotic effect in both breast cancer cell lines. The morphological changes indicative of apoptotic cell death were further confirmed by transmission electron microscopy providing evidence that the mitochondria were predominantly affected by RES (data not shown).

Resveratrol Disrupted Mitochondrial Function in Breast Cancer Cells. During chemical-induced apoptosis, early and pivotal events occur in the mitochondria that are often, although not always, associated with the collapse in $\Delta\Psi_m$ (Sun et al., 1999). To delineate this mechanism, we measured RES-induced alterations in $\Delta\Psi_m$ by using the mitochondrial selective lipophilic cation JC-1. In MDA-MB-231 and MCF-7 cells, RES exerts a dose-dependent decrease in the ratio of JC-1 red-green fluorescence intensity after 10

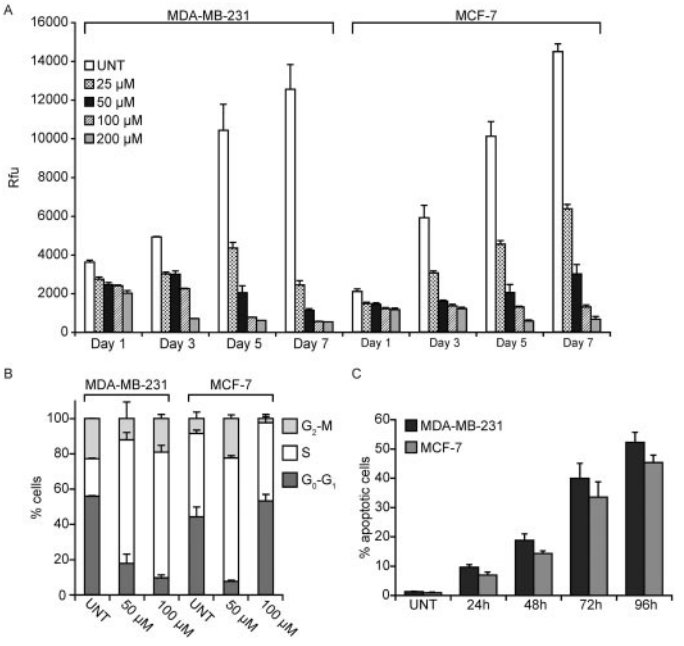

Fig. 1. Resveratrol engenders concentration- and time-dependent antiproliferation and apoptosis in breast cancer cells in vitro. A, cells were seeded at a density of 2.5×10^4/200 μl in a 96-well plate and treated with DMSO vehicle control (UNT) or 25, 50, 100, and 200 μM RES. Cell viability was measured using the CellTiter-Blue assay at the end of 1, 3, 5, and 7 days of treatment as described under *Materials and Methods*. B, cells seeded on 100-mm plates at a density of 5×10^6 cells were treated with DMSO (UNT) or 50 and 100 μM RES for 48 h. Nuclei were isolated from cells and stained with propidium iodide followed by flow cytometric analysis. The percentages of cells in G_0/G_1, S, and G_2-M phases of the cell cycle were analyzed and represented within the histograms. C, cells were seeded at a density of 2×10^5 cells/ml, treated with DMSO vehicle (UNT) or 100 μM RES for 24, 48, 72, or 96 h, stained with Hoechst 33528 and nuclear morphology examined by fluorescence microscopy. Cells exhibiting pyknotic nuclei and chromatin condensation were counted, and the number of apoptotic cells was determined as a percentage of the total number of cells in a viewing field. Value at each time point was averaged over five different viewing fields. Data (A, B, and C) represent means ± S.D. of triplicate samples. Results are representative of one of three independent experiments with similar results.

TABLE 1

Oral administration of resveratrol suppresses growth of an established MDA-MB-231 breast cancer xenograft in vivo

MDA-MB-231 cells resuspended in Matrigel were injected subcutaneously into the dorsal flank of *nu/nu* mice, and tumors were allowed to grow. Thirty-six mice per group were fed RES (50 mg/kg per day) in vehicle (Neobee M5 oil) or vehicle alone by oral gavage. At the end of 5 weeks of treatment, tumors were recovered and measured. Tumor volume was transformed to the log scale before analysis to obtain approximately normal distribution residuals and analyzed using a one-way analysis of variance test to detect statistical differences in tumor size among the groups. Data represent the average tumor volume in mm^3 assessed by caliper measurement ± S.E. Differences in tumor volume among the vehicle- and RES-treated groups were considered statistically significant at $P < 0.05$.

Group	Tumor Size	Standard Error	*n*	*P* Value
	mm^3			
Vehicle	630.96	103.86	36	0.003
50 mg/kg RES	307.62	52.3	36	

min of treatment, representing cells with rapidly depolarized mitochondria (Fig. 2, A and B). Significant depolarization with 2- to 10-fold decrease in $\Delta\Psi_m$ can be observed in both cell lines after RES treatment. Positive controls carbonyl cyanide p-trifluoromethoxyphenylhydrazone (FCCP; protonophore) and valinomycin (potassium ionophore) function as uncouplers of mitochondrial oxidative phosphorylation and significantly dissipate electrochemical gradients across the intermembrane space (Fig. 2, A and B). The RES-induced collapse of $\Delta\Psi_m$ could be due either to its effects on mitochondrion stability through an indirect mechanism and/or to direct interaction with the mitochondria.

We therefore determined whether RES might directly target mitochondria in a cell-free system to induce the collapse of $\Delta\Psi_m$. Freshly isolated mitochondria were incubated with JC-1 dye after treatment with various doses of RES, and the intensity of red fluorescence was monitored, with a decrease signifying the inability of the dye to form J-aggregates (red) in the mitochondria as a result of a loss of $\Delta\Psi_m$. RES directly causes a concentration-dependent decrease in $\Delta\Psi_m$ in the suspension of isolated mitochondria, which is rapid (within 10 min) and irreversible after drug removal (Fig. 2, C and D). In isolated mitochondria, the changes in $\Delta\Psi_m$ after RES treatment can be observed starting at considerably lower concentrations (Fig. 2C, compare with Fig. 2A), compared with whole cells. At 10 μM RES, the J-aggregates are almost undetectable in the isolated mitochondria, indicating complete loss of $\Delta\Psi_m$. Positive controls FCCP and sodium azide, which is an electron transport chain inhibitor, also significantly depolarize mitochondrial membranes. Thus, RES causes mitochondrial dysfunction, probably through its ability to directly target the mitochondria.

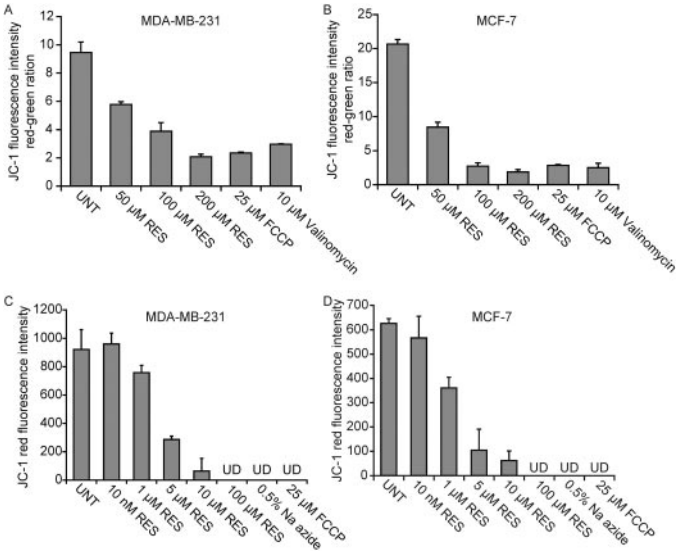

Fig. 2. Resveratrol causes loss of $\Delta\Psi_m$ in intact cells and isolated mitochondria. MDA-MB-231 cells (A) and MCF-7 cells (B) were treated with DMSO (UNT) or 50, 100, and 200 μM RES, 25 μM FCCP, and 10 μM valinomycin for 10 min. Cells in a suspension at 5×10^5 cells/ml were rinsed, stained with JC-1 dye, and monitored for changes in the red-green fluorescence ratio (red fluorescence derived from J-aggregates in the mitochondria − green fluorescence from monomeric JC-1 in the cytosol). C and D, mitochondrial fractions were isolated from MDA-MB-231 (C) and MCF-7 (D) cells as described under *Materials and Methods*. Protein concentrations were measured using the Bradford assay to determine equal amounts per sample. Isolated mitochondria were treated with DMSO (UNT) or 10 nM, 1 μM, 5 μM, 10 μM, and 100 μM RES, 0.5% sodium azide and 25 μM FCCP for 10 min and stained with JC-1. Changes in $\Delta\Psi_m$ were measured by monitoring JC-1 red fluorescence intensity; UD, undetectable. Data (A, B, C, and D) represent means ± S.D. of duplicate samples. Results are representative of one of three independent experiments with similar results.

Resveratrol Mediated Release of Apoptogenic Factors from the Mitochondria of MDA-MB-231 cells. Various apoptotic stimuli lead to changes in mitochondrial membrane permeability, resulting in loss of $\Delta\Psi_m$ and the subsequent release of apoptogenic factors, including cyt *c* and Smac/DIABLO. Western blot analysis was performed on cytosolic and mitochondrial fractions isolated from untreated or RES-treated breast cancer cells. In MDA-MB-231 cells, cyt *c* and Smac/DIABLO could be detected in the cytosolic compartment as early as 4 h after RES exposure (Fig. 3). Both proteins are progressively released into the cytosolic fraction in increasing amounts over 4 to 48h of RES treatment, after a loss in $\Delta\Psi_m$ seen much earlier, at 15 min after treatment. However, similar to our observations in other cancer models, RES could not provoke cyt *c* or Smac/DIABLO release from isolated mitochondria of breast cancer cells (data not shown), perhaps indicating a requirement for additional cytosolic factors (Sareen et al., 2006).

Resveratrol Activated Caspase-Dependent and -Independent Cell Death in MDA-MB-231 and MCF-7 Cells, Respectively. Mitochondrion- and death receptor-dependent apoptosis is known to be executed by the linkage activation of initiator caspases, which include caspases-2, -8, -9, -10, and -12 , and effector caspases, which include caspases-3, -6, and -7. We and others have established that loss of $\Delta\Psi_m$ and release of apoptogenic factors accompanies mitochondrion-dependent apoptosis induced by RES (Aggarwal et al., 2004; Sareen et al., 2006). To further determine the involvement of caspases in breast cancer cells upon RES-induced Ca^{2+} deregulation and mitochondria-mediated apoptosis, we examined cleavage of fluorogenic peptide substrates that mimic the target cleavage sites of caspases-2, -8, -9, and -3/7. It has been reported that MCF-7 cells lack caspase-3 activity because of a point mutation in the gene coding for this protein (Jänicke et al., 1998). As expected, RES was unable to induce caspase-3 as well as caspase-9 activation in this cell line (Fig. 4, A and B). However, a

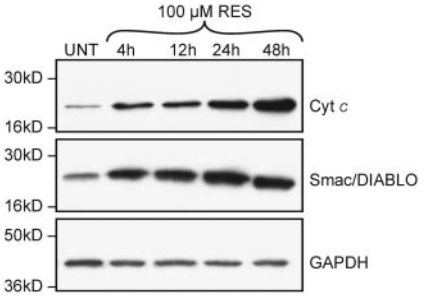

Fig. 3. RES provokes mitochondrial release of cytochrome c and Smac/DIABLO in MDA-MB-231 cells. Cells seeded on plates were treated with DMSO (UNT) or 100 μM RES for 4, 12, 24, and 48 h, washed and permeablilized in 0.04% digitonin extraction buffer. Cytosolic fractions free of mitochondria were prepared by differential centrifugation as described under *Materials and Methods*. Fifty micrograms of cytosolic fraction was processed for Western blotting, probed with antibody against cyt *c* (top) and Smac/DIABLO (center). GAPDH (bottom) immunostaining served as a loading control. Results are representative of one of two independent experiments with similar results.

demonstrable time-dependent increase in the activities of caspase-9 and -3 can be identified in RES treated MDA-MB-231 cells (Fig. 4, A and B). Slight increase in caspase-9 and -3 activities were already detectable 24 h after the addition of RES, although maximum activation of ~3- to 5-fold was observed after 72 h.

RES-induced apoptosis also could be regulated by the death-receptor pathway via early caspase-2 and -8 activation (Mohan et al., 2006). To address this possibility, cells were treated with RES and incubated with peptide substrates specific to caspase-2 and -8. RES was unable to induce either caspase-2 or -8 activation in MCF-7 and MDA-MB-231 cells compared with the untreated control (Fig. 4, C and D). This effect could not be attributed to MDA-MB-231 cells being refractory to activation of caspase-2 and -8 because the apoptotic inducers UV radiation, TG, and staurosporine provoked significant activation of the proteases. Caspase-2 activation could not be detected in MCF-7 cells in response to any apoptotic stimuli tested. Moreover, we did not observe cleavage and activation of procaspase-12, an ER stress-specific initiator caspase, upon RES treatment (data not shown).

Resveratrol Increased Intracellular Calcium Levels in Breast Cancer Cells. In many cases, an early and pivotal event in apoptosis is a Ca^{2+} influx through plasma membrane channels and/or release from the ER into the cytosol. RES has been demonstrated to enhance agonist-stimulated $[Ca^{2+}]_i$ increase in endothelial cells of the heart valve; however, there is no information about whether alteration of Ca^{2+} homeostasis plays a pivotal role during early RES-mediated cell death (Buluc and Demirel-Yilmaz, 2006). To determine whether this was an early event during RES-induced apoptosis, we first examined whether intracellular Ca^{2+} levels increased in log-phase MCF-7 cells after RES exposure using fura-2-AM in a spectrofluorometric assay.

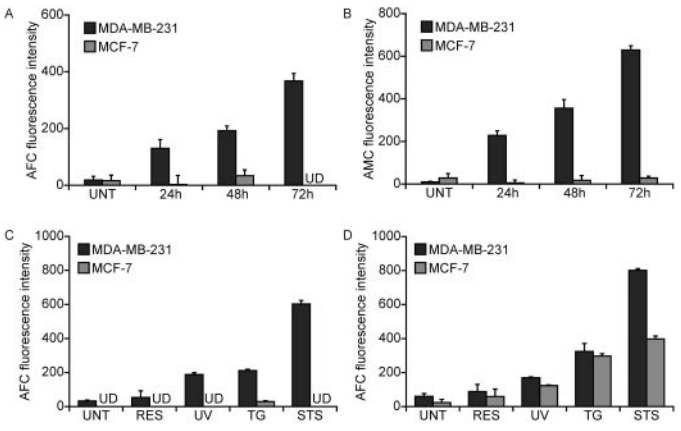

Fig. 4. Resveratrol induces caspase-dependent apoptosis in MDA-MB-231 cells and caspase-independent apoptosis in MCF-7 cells. A and B, MDA-MB-231 and MCF-7 cultures were treated with DMSO (UNT) for 72 h or 100 μM RES for 24, 48, and 72 h and lysed, and caspase-9 (A) and caspase-3 (B) activities were measured spectrofluorometrically using respective peptide substrates. The graphs show relative fluorescence intensity of free AFC (A) and AMC (B) released upon enzymatic activation. C and D, cells were treated with DMSO control, 100 μM RES, 1 μM TG, 1 μM staurosporine (STS), or exposed to 200 J/m^2 UV radiation, lysed, and caspase-2 (C) and caspase-8 (D) activities were measured 24 h later using fluorometric peptide substrates. The graphs show relative fluorescence intensity of free AFC released. The lysates were adjusted for equal protein concentrations using the Bradford assay. Data (A, B, C, and D) represent means ± S.D. of duplicate samples. Results are representative of one of three independent experiments with similar results.

Eight minutes after treatment, RES and ionomycin caused ~3- and 1.7-fold increases in $[Ca^{2+}]_i$, respectively, compared with the vehicle control (Fig. 5A).

This result was substantiated by performing live cell Ca^{2+}-imaging on a BD Pathway Bioimaging microscopy system with fura-2 loaded MCF-7 cells. Before drug addition, cells analyzed in different regions of interest (ROI) started with comparable basal fura-2 fluorescence, reflecting resting intracellular Ca^{2+} levels. After RES addition, an elevation in intracellular Ca^{2+} levels was observed within different ROI of MCF-7 cells (Fig. 5B), supporting data from our spectrofluorometric assay. The same results were obtained from similar experiments conducted with MDA-MB-231 cells. Figure 5 further illustrates the kinetics of RES-induced changes in $[Ca^{2+}]_i$ and provides an indication of the source of Ca^{2+} release. The basal $[Ca^{2+}]_i$ level in MDA-MB-231 cells was 142 ± 39 (mean ± S.E.) nM; n = 36. At 10 to 35 s after exposure to RES, cells exhibited a significant increase of ~2- to 4-fold in $[Ca^{2+}]_i$, with peak levels at 476 ± 96 nM, after which time the levels returned to approximately 283 ± 44 nM, although they never reached the basal levels (Fig. 5C; images with inset and graph). It is noteworthy that, beginning at ~240 s after RES exposure, there was a second gradual rise in $[Ca^{2+}]_i$ that saturated at ~900 s with a peak value of 422 ± 68 nM and did not return to resting levels within the experimental time of 45 min. The basal level of $[Ca^{2+}]_i$ (128 ± 29 nM; n = 28) was not affected significantly in both cell lines upon treatment with the DMSO vehicle control (Fig. 5E, top right). To ensure that the RES-induced changes in $[Ca^{2+}]_i$ detected by fura-2 are Ca^{2+}-specific, cells preloaded with the intracellular Ca^{2+} chelator BAPTA-AM were evaluated by imaging. BAPTA-AM increased the cytosolic Ca^{2+} buffering capacity of the cells; the magnitude of the $[Ca^{2+}]_i$ rise after RES exposure was almost completely attenuated (Fig. 5E, bottom right) Untreated or BAPTA-AM-loaded cells did not show fluctuations in basal Ca^{2+} levels during the time course of the experiment.

Because the ER is a major intracellular reservoir of Ca^{2+}, we tested whether the Ca^{2+} signal evoked by RES originated from this organelle by employing TG, a known specific mobilizer of the ER Ca^{2+} stores that causes rapid and transient increases in $[Ca^{2+}]_i$. If RES exposure led to release of Ca^{2+} stored in the ER, then TG administration should not cause additional Ca^{2+} release. If the sequence of drug administration were reversed, additional Ca^{2+} release should not be observed. TG alone evoked a typical Ca^{2+} response of ~3- to 4-fold over basal $[Ca^{2+}]_i$ 35 s after exposure; cells reached a maximal concentration of 454 ± 82 nM (Fig. 5D, images and graph). When TG was added to cells after RES, none of the cells that initially responded to RES exhibited a rise in intracellular Ca^{2+} levels after TG administration (Fig. 5E, bottom left). Likewise, when RES was added after TG-induced depletion of ER Ca^{2+} stores, no measurable spike was observed (Fig. 5E, top left). However, the second gradual rise in $[Ca^{2+}]_i$ was unaffected by RES addition. We noted that the increase in $[Ca^{2+}]_i$ (3–4-fold over basal levels, Fig. 5C) observed after exposure to RES was comparable with that elicited by TG (Fig. 5D), further suggesting that the two agents may mobilize the same ER pool of Ca^{2+}. The percentage of cells responding to RES and TG in a given culture was similar, averaging ~80%.

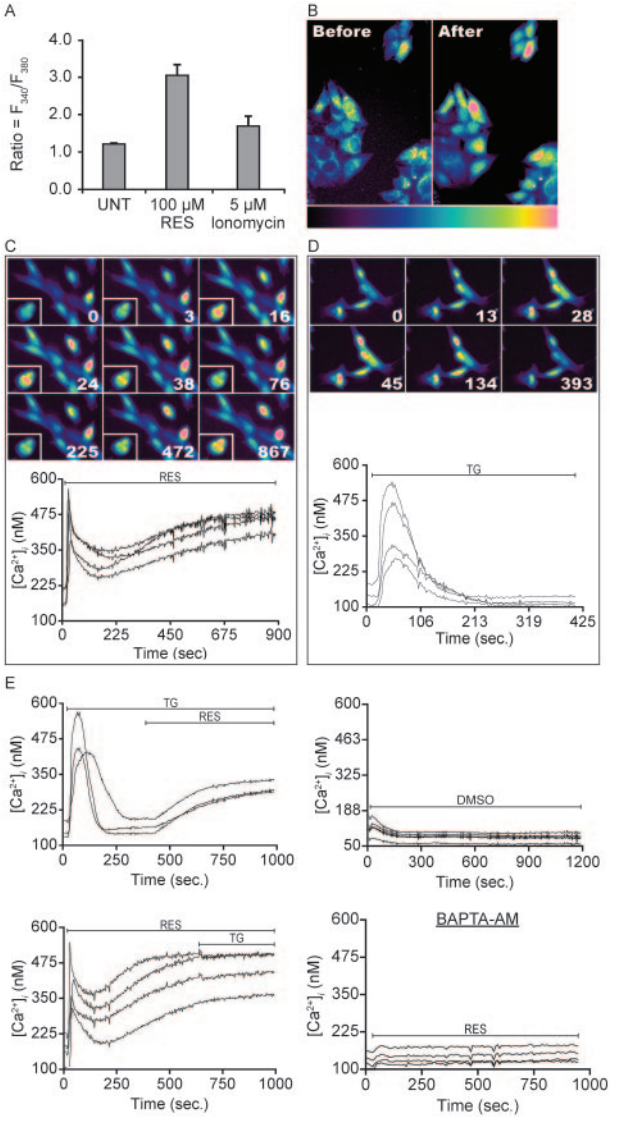

Fig. 5. Resveratrol increases intracellular calcium levels in breast cancer cells. MCF-7 and MDA-MB-231 cells seeded at 2×10^5 cells in 96-well plates were loaded with fura-2-AM. A, DMSO control (UNT), 100 μM RES, or 5 μM ionomycin was added to MCF-7 cells after basal measurements were made on a spectrofluorometer. After drug addition, measurements were made every 60 s for 10 min. Graph depicts changes in $[Ca^{2+}]_i$ at 6 min after drug addition by measuring the fluorescence intensity ratio (F^{340}/F^{380}) of the Ca^{2+}-bound/ Ca^{2+}-free fura-2. Histograms represent means ± S.D. of triplicate samples and represent one of at least two independent experiments. B, live cell microscopy was performed in MCF-7 cells to observe alterations in intracellular Ca^{2+} before and after addition of 100 μM RES. Cells representative of an average response of the entire population before and drug treatment were selected and shown as pseudocolored ROI images, along with a reference pseudocolor scale depicting increasing $[Ca^{2+}]_i$ concentration from left to right. C–E, live cell microscopy was performed in MDA-MB-231 cells to measure changes in $[Ca^{2+}]_i$ in response to 100 μM RES and 5 μM TG. The number in the bottom right corner of each fluorescent pseudocolored image represents the time in seconds after drug addition (C and D). The inset images (C) depict a cell with a maximal response in $[Ca^{2+}]_i$ to RES treatment. The Ca^{2+} mobilization responses to RES (C) and TG (D) are also displayed in graphs showing changes in $[Ca^{2+}]_i$ concentration (nanomolar) after the measured F^{340}/F^{380} ratio was calibrated with standard solutions to make the required conversions. The line segment on top of the graph depicts the period of drug stimulation. Each trace represents the change in $[Ca^{2+}]_i$ of an individual ROI (2–4 cells) selected over time; each graph is representative of one of at least three independent experiments. E, top left, representative Ca^{2+} mobilization traces upon sequential exposure of cells to 5 μM TG and 100 μM RES. E, bottom left, change in $[Ca^{2+}]_i$ upon addition of 100 μM RES followed by 5 μM TG exposure after near saturation of the biphasic RES response. E, top right, a trace of the cells treated with DMSO vehicle control. E, bottom right, 20 μM BAPTA-AM was coloaded with fura-2-AM, and the Ca^{2+} mobilization response was measured in response to 100 μM RES treatment.

Resveratrol Activateed a Calpain-Dependent Apoptotic Pathway in MCF-7 Cells. Despite the lesion in the intrinsic mitochondrial apoptotic pathway, MCF-7 cells undergo apoptosis in response to RES at an IC_{50} similar to that of MDA-MB-231 cells that express caspase-3. The rise in $[Ca^{2+}]_i$ and the resulting Ca^{2+} overload is thought to activate Ca^{2+}-dependent proteases, such as calpains, leading to structural damage and eventually cell death in certain neuronal models of apoptosis (Liu et al., 2004; Bano et al., 2005). However, little is known about the involvement of calpains in tumor cell death. To avoid the invasive procedure of cellular lysates, we performed the calpain activity assay in intact MCF-7 cells by using a cell-permeable and fluorescent calpain substrate, S-LLVY-AMC. In addition, MCF-7 cells provided an opportunity to unmask a calpain-dependent apoptotic pathway as a result of the absence of an active caspase-dependent intrinsic mitochondrial apoptotic pathway. Calpain activity in RES-treated cells is early and significantly higher compared with the basal levels observed in DMSO-treated control cells, measured at 15 min after drug addition (Fig. 6A). As expected, in samples pretreated with the intracellular Ca^{2+}-chelator BAPTA-AM and calpain inhibitors with various specificities (PD 150606, MDL 28170, and SJA 6017), the RES-induced increase in calpain activity was almost completely blocked. This bolsters evidence that the fluorescent signal measured in this assay was dependent upon an increase in intracellular Ca^{2+} and is specific for calpain activity. The RES-induced increase in calpain activity remains substantial at 36 h after treatment (data not shown).

Upon apoptotic insult, the mitochondria play an essential role in buffering nontoxic loads of Ca^{2+}, and the mPTP provides a fast Ca^{2+} extrusion mechanism in response to abnormally high levels that accumulate in mitochondria during apoptosis. Some mPTP antagonists, such as CsA, have been shown to inhibit this process, either through specific inhibition of cyclophilin D or through inhibition of calcineurin phosphatase activity (Montero et al., 2004). To determine whether mitochondrial Ca^{2+} release from mPTP was involved in RES-induced calpain activation, we employed the mPTP inhibitor CsA. The increase in AMC fluorescence, indicating calpain activation, can be seen in RES-treated MCF-7 cells (Fig. 6B). It is noteworthy that RES-induced calpain activation was completely abolished by CsA pretreatment. The fact that CsA prevented calpain activation suggests that mPTP somehow mediated the observed calpain activation after RES treatment.

Degradation of Calpain-Specific Protein Substrates Contributed to Resveratrol-Induced MCF-7 Cell Death. To further characterize the mechanism of calpain-dependent cell death initiated by RES, we investigated the in vivo cleavage pattern of calpain protein substrates in MCF-7 cell lysates by Western analysis (Fig. 7). Fodrin (α-spectrin) is a known substrate of caspase-3 as well as calpains. Although caspases and calpains share a number of substrates, their cleavage during treatment with RES in MCF-7 cells would indicate calpain activity, because effector caspases are

not activated in this model. Over a period of 24 to 48 h, in the presence of RES, specific calpain-dependent processing of fodrin was detected, evidenced by disappearance of the 240/280-kDa native band. However, in the presence of RES and the calpain inhibitor SJA 6017, the native fodrin remains intact at all times and the 145/150-kDa cleavage was not observed (Fig. 6B, top). As expected, no caspase-3-mediated 120 kDa breakdown product was observed. Mechanisms that regulate the cellular extrusion of Ca^{2+} could potentially rectify the RES-induced Ca^{2+} increase. To determine whether RES-activated calpain can target such a mechanism, we explored the cleavage pattern of Ca^{2+} pumps in the presence of a known calpain inhibitor. Beginning at 24 h after RES treatment, native PMCA1a/b (130–134-kDa) was cleaved in a calpain-dependent manner in MCF-7 cells (Fig. 6B, middle).

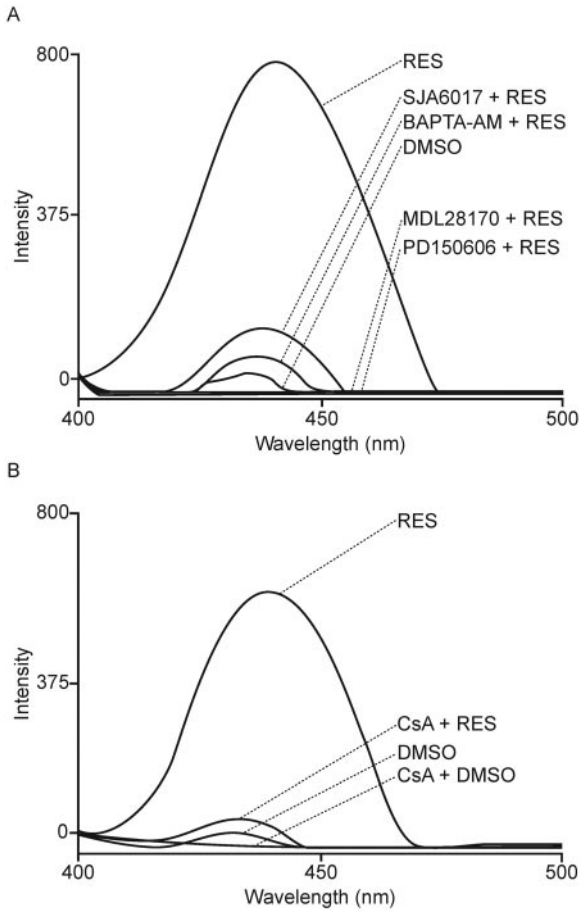

Fig. 6. Resveratrol activates calpain as a function of mPTP opening in MCF-7 cells. A, MCF-7 cells were harvested and washed. For each condition, 2.5×10^5 cells/ml were left untreated or pretreated with intracellular Ca^{2+}-chelator BAPTA-AM, and calpain inhibitors PD 150606, SJA 6017, and MDL 28170 for 30 to 60 min. DMSO or 100 μM RES was added to untreated or pretreated cell suspension followed by the fluorogenic calpain substrate S-LLVY-AMC. Subsequently, calpain activity was monitored as a function of time by measuring the increase in fluorescence intensity of free AMC using a spectrofluorometer. The graph depicts calpain activity curves for different conditions plotted at 15 min after drug treatment. B, MCF-7 cells prepared and assayed for calpain activity described in A. Cells were left untreated or pretreated with the mPTP inhibitor, CsA for 30 to 45 min. Cells were then treated with DMSO or RES followed by substrate addition. Free AMC fluorescence generated was measured, and curves were plotted at 15 min after treatment. Data (A and B) depict a representative curve obtained from duplicate points measured for each condition. The experiment was repeated three times with similar results.

Cotreating cells with the calpain inhibitor SJA 6017 in the presence of RES prevented PMCA1a/b cleavage. However, there was no evidence of calpain-dependent PMCA4 degradation in the presence of RES (data not shown).

Discussion

In search for novel strategies for further management of breast cancer, we have attempted to identify the molecular mechanisms involved in RES-induced apoptosis, both caspase-dependent and -independent. To the best of our knowledge, this is one of the first studies to describe the chemotherapeutic effects of RES-induced alterations in Ca^{2+} homeostasis.

In the present study, we illustrate the in vivo anticancer efficacy of RES against breast cancer tumor growth in the MDA-MB-231 xenograft model without any toxicity. Data from preliminary studies suggests that RES exhibits similar efficacy against the MCF-7 xenograft model. In vitro studies demonstrate that RES exerts dose- and time-dependent antiproliferative and proapoptotic effects in MCF-7 and MDA-MB-231 cells, thus decreasing cell viability. The antiproliferative activity of RES against tumor cell lines of different origins has been extensively characterized and attributed to inhibition of various factors, such as cycloxygenase-1 and -2, ribonucleotide reductase, nuclear transcription factor-κB, and its target genes (Aggarwal et al., 2004; Delmas et al., 2006). In contrast to in vitro data on enzyme inhibition, the RES anticancer effect in vivo may involve deregulation of multiple targets, promoting parallel or overlapping cascades of events inducing cell cycle arrest and eventually apoptosis.

Although RES has been shown to instigate apoptosis in various cancer models, data from our studies show that mitochondria were significantly affected shortly after RES treatment and are likely to play a central role in mediating apoptosis. RES treatment rapidly dissipates $\Delta\Psi_m$ in whole cells, and lower concentrations of RES were sufficient to influence a loss of $\Delta\Psi_m$ in isolated mitochondria, indicating the possibility of a novel RES target protein in the mitochondria. Opening of the mPTP, composed of the adenine-nucleotide

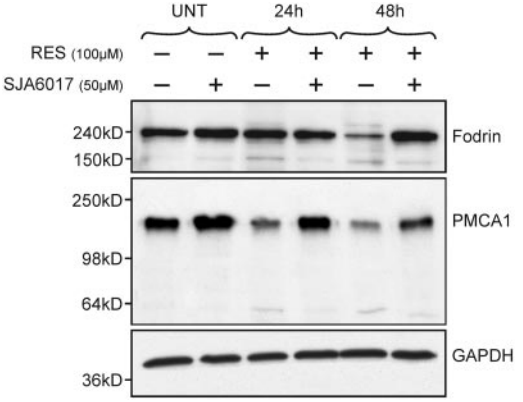

Fig. 7. Resveratrol induces degradation of calpain-specific protein substrates in MCF-7 cells. Cells seeded on plates were treated with DMSO (UNT) or 100 μM RES alone or in combination with the calpain inhibitor SJA 6017 for a period of 24 and 48 h. Cultures were scraped, washed, and lysed, and protein concentration was then determined in cell lysates using the Bradford assay. Twenty five micrograms of protein was processed for Western blotting and probed with antibodies specific for α-fodrin or PMCA1. GAPDH immunostaining served as a loading control. The experiments were repeated three times with similar results.

translocator and the voltage-dependent anion channel, has been suggested to play important roles in mediating loss of $\Delta\Psi_m$ and cyt *c* release (Martinou et al., 2000; Petronilli et al., 2001). Whether resveratrol's ability to directly target mitochondria and cause a loss of $\Delta\Psi_m$ in breast cancer cells is somehow linked through these protein complexes requires further investigation.

Disruption of $\Delta\Psi_m$ leading to mitochondrial permeabilization commonly accompanies or precedes release of cyt *c* and Smac/DIABLO into the cytoplasm, leading to formation of an active apoptosome complex and activation of caspase-9, which then activates the executioner caspase-3 to orchestrate apoptosis (Green, 2005). We demonstrate that RES triggered release of cyt *c* and Smac/DIABLO from mitochondria of MDA-MB-231 cells, which precedes the activation of caspase-9 and -3, confirming previous findings from other groups in tumor cell lines of different origins (Aggarwal et al., 2004; Jiang et al., 2005; Pozo-Guisado et al., 2005). Although the precise mechanism that mediates the release of cyt *c* and Smac/DIABLO from the mitochondria is unclear, apoptosis-associated mitochondrial events induced by RES in many cancer cell types have been shown to be facilitated by the altered expression and mitochondrial localization of apoptotic regulators, such as down-modulation of the antiapoptotic proteins Bcl-2 and Bcl-X_L and up-regulation and mitochondrial translocation of pro-apoptotic Bax and Bak (Mahyar-Roemer et al., 2002; Jiang et al., 2005; Pozo-Guisado et al., 2005). As anticipated, activation of caspase-9 and -3 was not detectable upon RES treatment of MCF-7 cells. Alternatively, extrinsic death receptor mediated apoptosis proceeding through the activation of initiator caspases-2 and -8 has been elicited by RES (Delmas et al., 2003; Mohan et al., 2006). However, the absence of caspase-2 and -8 activation in response to RES treatment of MDA-MB-231 and MCF-7 cells indicates that the death receptor pathway is not a likely early mechanism of RES-induced apoptosis in these cells.

Our results reveal that RES evokes a rapid and biphasic increase in $[Ca^{2+}]_i$ in both breast cancer cell lines, supporting our hypothesis that homeostatic mechanisms for regulating cellular Ca^{2+} possibly play a central role during RES-induced apoptosis. The initial rise seems to be dependent upon the ability of RES to stimulate the TG-sensitive Ca^{2+} stores, likely the ER. The second rise is possibly due to the release of buffered Ca^{2+} from the mitochondrial stores or extracellular influx of Ca^{2+} by plasma membrane channels. To confirm the source of this RES-induced Ca^{2+} release, organelle-specific Ca^{2+}-sensitive indicators need to be employed.

During apoptosis, the amplitude of the initial $[Ca^{2+}]_i$ elevation is usually within the range of nonlethal stimulations, whereas the subsequent rise leading to a massive Ca^{2+} accumulation requires additional mechanisms to terminally deregulate cellular Ca^{2+} handling (Orrenius et al., 2003). Our results demonstrate for the first time that RES treatment induces calpain activation in MCF-7 cells, which can be blocked by active-site calpain inhibitors and BAPTA-AM. Because no difference in the substrate specificity of the calpain isozymes has been found, considering the level of RES-induced elevation in $[Ca^{2+}]_i$, we conclude that RES at least activated μ-calpain and possibly also other calpains. In the present study, activated calpain targets cytoskeletal proteins such as fodrin and the high-affinity Ca^{2+} pump, PMCA1, for degradation in cells exposed to RES. The calpain-dependent degradation of PMCA1 possibly prevents it from functioning and maintaining Ca^{2+} homeostasis. This, in turn, could facilitate Ca^{2+} leakage down its concentration gradient into the cytosol, providing a secondary sustained Ca^{2+} elevation that results in proteolytic degradation and ultimately apoptosis. Coadministration of RES and calpain inhibitor successfully abrogates calpain-induced fodrin and PMCA1 cleavage. Previously, in vitro studies have shown PMCA1, 2, and 4 to be susceptible to calpain degradation with differing sensitivities, and the erythrocyte calcium pump has been shown to be a preferred substrate of calpain in vivo (Guerini et al., 2003). To the best of our knowledge, this is the first study demonstrating an in vivo calpain-induced cleavage of PMCA1 in response to RES.

The mitochondria play an essential role in buffering physiological loads of Ca^{2+} upon insult, whereas the mPTP provides a fast Ca^{2+} extrusion mechanism in response to abnormally high levels of Ca^{2+} that accumulate in mitochondria during apoptosis. RES has been demonstrated to promote Ca^{2+}-mediated mPTP opening by activating a Ca^{2+}-induced Ca^{2+} release (CICR) from rat liver mitochondria, and this effect was completely inhibited by CsA (Tian et al., 2006). It is noteworthy that we observed that RES-induced calpain activation was significantly inhibited in the presence of CsA,

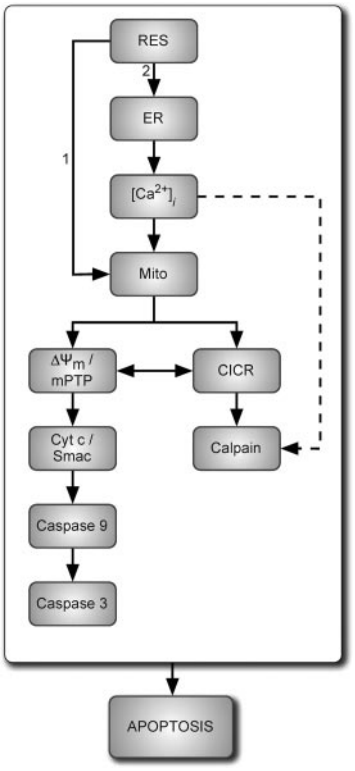

Fig. 8. Mechanisms of resveratrol-induced apoptosis. 1, RES targets the mitochondria, resulting in mitochondrial depolarization that is frequently associated with mPTP opening. Subsequent mitochondrial release of cyt *c* and Smac/DIABLO leads to activation of caspase-9 and -3, resulting in apoptosis. 2, RES targets the ER, causing an elevation of $[Ca^{2+}]_i$ that is biphasic in nature. The initial rise in cytoplasmic Ca^{2+} is probably buffered by the mitochondria. The second phase is probably due to the release of buffered mitochondrial Ca^{2+} to the cytoplasm, commonly known as CICR. There is evidence that CICR can either precede or follow mitochondrial depolarization. Subsequent calpain activation may be the result of the first (dotted arrow) or second phase of rise in $[Ca^{2+}]_i$. Active calpain is responsible for proteolysis of its substrates, ultimately leading to apoptosis.

suggesting that calpain activation may be a postmitochondrial event. The precise mechanism of this mPTP inhibition is still elusive, although it is possible that CsA enhances the mitochondrial uptake and retention of Ca^{2+} and thereby prevents calpain activation during recovery, as indicated in a recent study in which CsA prevented calpain activation after microcystin-induced cell death in hepatocytes (Ding et al., 2002).

These results support the hypothesis that RES is a multifaceted molecule capable of directly targeting the mitochondria and activating the intrinsic mitochondrial caspase-dependent form of apoptosis. In addition, RES targets the thapsigargin-sensitive ER Ca^{2+} stores to cause an elevation of intracellular Ca^{2+} levels in both breast cancer cell lines. Subsequent Ca^{2+}-dependent activation of calpain is observed. This mechanism of apoptosis may be especially relevant in tumors lacking caspase-3 activity (Devarajan et al., 2002). Thus, it is likely that resveratrol's pro-apoptotic mechanism involves deregulation of multiple targets associated with the mitochondria and ER, leading to the activation of different enzymatic cascades described in Fig. 8.

Together, these data for the first time link changes in Ca^{2+} homeostasis to the RES-mediated initiation of apoptosis. Sustained elevations in intracellular Ca^{2+}, therefore, might serve as a universal cell death signal that can be exploited for antitumor therapy. Differences in expression of a RES target and/or Ca^{2+} regulatory mechanisms in cancer versus normal cells may allow RES to induce apoptosis selectively in breast cancer cells. Identification of a putative RES mitochondrial and/or ER target could lead to the synthesis of more efficacious apoptotic anticancer agents. We hope that our findings will aid in the development of therapeutic strategies for the use of RES as a nontoxic alternative to conventional anticancer therapies for breast cancer.

Acknowledgments

We thank Joshua Harder for help in preparation of the manuscript and Dr. Mary J. Lindstrom for conducting the statistical analyses.

References

Aggarwal BB, Bhardwaj A, Aggarwal RS, Seeram NP, Shishodia S, and Takada Y (2004) Role of resveratrol in prevention and therapy of cancer: preclinical and clinical studies. *Anticancer Res* **24:**2783–2840.

Ashkenazi A and Dixit VM (1998) Death receptors: signaling and modulation. *Science* **281:**1305–1308.

Banerjee S, Bueso-Ramos C, and Aggarwal BB (2002) Suppression of 7,12-dimethylbenz(a)anthracene-induced mammary carcinogenesis in rats by resveratrol: role of nuclear factor-kappaB, cyclooxygenase 2, and matrix metalloprotease 9. *Cancer Res* **62:**4945–4954.

Bano D, Young KW, Guerin CJ, Lefeuvre R, Rothwell NJ, Naldini L, Rizzuto R, Carafoli E, and Nicotera P (2005) Cleavage of the plasma membrane Na^+/Ca^{2+} exchanger in excitotoxicity. *Cell* **120:**275–285.

Bhat KP, Lantvit D, Christov K, Mehta RG, Moon RC, and Pezzuto JM (2001) Estrogenic and antiestrogenic properties of resveratrol in mammary tumor models. *Cancer Res* **61:**7456–7463.

Bradamante S, Barenghi L, and Villa A (2004) Cardiovascular protective effects of resveratrol. *Cardiovasc Drug Rev* **22:**169–188.

Buluc M and Demirel-Yilmaz E (2006) Resveratrol decreases calcium sensitivity of vascular smooth muscle and enhances cytosolic calcium increase in endothelium. *Vascul Pharmacol* **44:**231–237.

Delmas D, Lancon A, Colin D, Jannin B, and Latruffe N (2006) Resveratrol as a chemopreventive agent: a promising molecule for fighting cancer. *Curr Drug Targets* **7:**423–442.

Delmas D, Rebe C, Lacour S, Filomenko R, Athias A, Gambert P, Cherkaoui-Malki M, Jannin B, Dubrez-Daloz L, Latruffe N, et al. (2003) Resveratrol-induced apoptosis is associated with Fas redistribution in the rafts and the formation of a death-inducing signaling complex in colon cancer cells. *J Biol Chem* **278:**41482–41490.

Devarajan E, Sahin AA, Chen JS, Krishnamurthy RR, Aggarwal N, Brun AM, Sapino A, Zhang F, Sharma D, Yang XH, et al. (2002) Down-regulation of caspase-3 in breast cancer: a possible mechanism for chemoresistance. *Oncogene* **21:**8843–8851.

Ding WX, Shen HM, and Ong CN (2002) Calpain activation after mitochondrial permeability transition in microcystin-induced cell death in rat hepatocytes. *Biochem Biophys Res Commun* **291:**321–331.

Garvin S, Ollinger K, and Dabrosin C (2006) Resveratrol induces apoptosis and inhibits angiogenesis in human breast cancer xenografts in vivo. *Cancer Lett* **231:**113–122.

Green DR (2005) Apoptotic pathways: ten minutes to dead. *Cell* **121:**671–674.

Green DR and Reed JC (1998) Mitochondria and apoptosis. *Science* **281:**1309–1312.

Grynkiewicz G, Poenie M, and Tsien RY (1985) A new generation of Ca^{2+} indicators with greatly improved fluorescence properties. *J Biol Chem* **260:**3440–3450.

Guerini D, Pan B, and Carafoli E (2003) Expression, purification, and characterization of isoform 1 of the plasma membrane Ca^{2+} pump: focus on calpain sensitivity. *J Biol Chem* **278:**38141–38148.

Guttmann RP and Johnson GV (1998) Oxidative stress inhibits calpain activity in situ. *J Biol Chem* **273:**13331–13338.

Hambrock A, de Oliveira Franz CB, Hiller S, Grenz A, Ackermann S, Schulze DU, Drews G, and Osswald H (2007) Resveratrol binds to the sulfonylurea receptor (SUR) and induces apoptosis in a SUR subtype-specific manner. *J Biol Chem* **282:**3347–3356.

Harwood SM, Yaqoob MM, and Allen DA (2005) Caspase and calpain function in cell death: bridging the gap between apoptosis and necrosis. *Ann Clin Biochem* **42:**415–431.

Jang M, Cai L, Udeani GO, Slowing KV, Thomas CF, Beecher CW, Fong HH, Farnsworth NR, Kinghorn AD, Mehta RG, et al. (1997) Cancer chemopreventive activity of resveratrol, a natural product derived from grapes. *Science* **275:**218–220.

Jänicke RU, Sprengart ML, Wati MR, and Porter AG (1998) Caspase-3 is required for DNA fragmentation and morphological changes associated with apoptosis. *J Biol Chem* **273:**9357–9360.

Jemal A, Siegel R, Ward E, Murray T, Xu J, Smigal C, and Thun MJ (2006) Cancer statistics, 2006. *CA Cancer J Clin* **56:**106–130.

Jiang H, Zhang L, Kuo J, Kuo K, Gautam SC, Groc L, Rodriguez AI, Koubi D, Hunter TJ, Corcoran GB, et al. (2005) Resveratrol-induced apoptotic death in human U251 glioma cells. *Mol Cancer Ther* **4:**554–561.

Kim YA, Choi BT, Lee YT, Park DI, Rhee SH, Park KY, and Choi YH (2004) Resveratrol inhibits cell proliferation and induces apoptosis of human breast carcinoma MCF-7 cells. *Oncol Rep* **11:**441–446.

Lin HY, Lansing L, Merillon JM, Davis FB, Tang HY, Shih A, Vitrac X, Krisa S, Keating T, Cao HJ, et al. (2006) Integrin alphaVbeta3 contains a receptor site for resveratrol. *FASEB J* **20:**1742–1744.

Liu X, Van Vleet T, and Schnellmann RG (2004) The role of calpain in oncotic cell death. *Annu Rev Pharmacol Toxicol* **44:**349–370.

Mahyar-Roemer M, Kohler H, and Roemer K (2002) Role of Bax in resveratrol-induced apoptosis of colorectal carcinoma cells. *BMC Cancer* **2:**27.

Martinou JC, Desagher S, and Antonsson B (2000) Cytochrome c release from mitochondria: all or nothing. *Nat Cell Biol* **2:**E41–E43.

Mohan J, Gandhi AA, Bhavya BC, Rashmi R, Karunagaran D, Indu R, and Santhoshkumar TR (2006) Caspase-2 triggers Bax-Bak-dependent and -independent cell death in colon cancer cells treated with resveratrol. *J Biol Chem* **281:**17599–17611.

Montero M, Lobaton CD, Gutierrez-Fernandez S, Moreno A, and Alvarez J (2004) Calcineurin-independent inhibition of mitochondrial Ca^{2+} uptake by cyclosporin A. *Br J Pharmacol* **141:**263–268.

Orrenius S, Zhivotovsky B, and Nicotera P (2003) Regulation of cell death: the calcium-apoptosis link. *Nat Rev Mol Cell Biol* **4:**552–565.

Petronilli V, Penzo D, Scorrano L, Bernardi P, and Di Lisa F (2001) The mitochondrial permeability transition, release of cytochrome c and cell death. Correlation with the duration of pore openings in situ. *J Biol Chem* **276:**12030–12034.

Potter DA, Tirnauer JS, Janssen R, Croall DE, Hughes CN, Fiacco KA, Mier JW, Maki M, and Herman IM (1998) Calpain regulates actin remodeling during cell spreading. *J Cell Biol* **141:**647–662.

Pozo-Guisado E, Merino JM, Mulero-Navarro S, Lorenzo-Benayas MJ, Centeno F, Alvarez-Barrientos A, and Fernandez-Salguero PM (2005) Resveratrol-induced apoptosis in MCF-7 human breast cancer cells involves a caspase-independent mechanism with downregulation of Bcl-2 and NF-kappaB. *Int J Cancer* **115:**74–84.

Robinson JA, Jenkins NS, Holman NA, Roberts-Thomson SJ, and Monteith GR (2004) Ratiometric and nonratiometric Ca^{2+} indicators for the assessment of intracellular free Ca^{2+} in a breast cancer cell line using a fluorescence microplate reader. *J Biochem Biophys Methods* **58:**227–237.

Sareen D, van Ginkel PR, Takach JC, Mohiuddin A, Darjatmoko SR, Albert DM, and Polans AS (2006) Mitochondria as the primary target of resveratrol-induced apoptosis in human retinoblastoma cells. *Invest Ophthalmol Vis Sci* **47:**3708–3716.

Sasaki T, Kikuchi T, Yumoto N, Yoshimura N, and Murachi T (1984) Comparative specificity and kinetic studies on porcine calpain I and calpain II with naturally occurring peptides and synthetic fluorogenic substrates. *J Biol Chem* **259:**12489–12494.

Savouret JF and Quesne M (2002) Resveratrol and cancer: a review. *Biomed Pharmacother* **56:**84–87.

Sun XM, MacFarlane M, Zhuang J, Wolf BB, Green DR, and Cohen GM (1999) Distinct caspase cascades are initiated in receptor-mediated and chemical-induced apoptosis. *J Biol Chem* **274:**5053–5060.

Tian XM, Ma XD, and Yan F (2006) Resveratrol promotes Ca^{2+} -induced Ca^{2+} release from rat liver cell mitochondria mediated by Ca^{2+}. *Nan Fang Yi Ke Da Xue Xue Bao* **26:**910–913.

Address correspondence to: Dr. Arthur S. Polans, Department of Ophthalmology and Visual Sciences, School of Medicine and Public Health, Rm. K6/466 Clinical Sciences Center, 600 Highland Avenue, Madison, WI 53792. E-mail: aspolans@wisc.edu